analytical performance. Special attention should be given to the construction of these electrodes (in comparison to readily available glassy-carbon substrates). These (and similar) composite materials are thus expected to play a growing role in stripping analysis.

Registry No. C, 7440-44-0; Hg, 7439-97-6; Cd, 7440-43-9; Cu, 7440-50-8; Pb, 7439-92-1; H_2O, 7732-18-5.

REFERENCES

(1) Wang, J. *Stripping Analysis: Principles, Instrumentation and Applications*; VCH: Deerfield Beach, FL, 1985.
(2) Florence, T. M. *J. Electroanal. Chem. Interfacial Electrochem.* **1970**, *27*, 273-281.
(3) Harman, A. R.; Baranski, A. S. *Anal. Chim. Acta* **1990**, *239*, 35-46.
(4) Bond, A. M.; Luscombe, D. L.; Tan, S. N.; Walter, F. L. *Electroanalysis* **1990**, *2*, 195-202.
(5) Wang, J.; Tuzhi, P.; Zadeli, J. *Anal. Chem.* **1987**, *59*, 2119-2122.
(6) Wong, D. K. Y.; Ewing, A. G. *Anal. Chem.* **1990**, *62*, 2697-2702.
(7) Schulze, G.; Frenzel, W. *Anal. Chim. Acta* **1984**, *159*, 95-103.
(8) Huilliang, J.; Hua, C.; Jagner, D.; Renman, L. *Anal. Chim. Acta* **1987**, *193*, 61.
(9) Sottery, J. P.; Anderson, C. W. *Anal. Chem.* **1987**, *59*, 140-144.
(10) Tallman, D. E.; Petersen, S. L. *Electroanalysis* **1990**, *2*, 499-510.
(11) Wang, J.; Brennsteiner, A.; Sylwester, A. P. *Anal. Chem.* **1990**, *62*, 1102-1104.
(12) Davis, B. K.; Weber, S. G.; Sylwester, A. P. *Anal. Chem.* **1990**, *62*, 1000-1003.
(13) (a) Sylwester, A. P.; Aubert, J. H.; Rand, P. B.; Arnold, C., Jr.; Clough, R. L. *Polym. Mater. Sci. Eng.* **1987**, *57*, 113-118. (b) U.S. Patent 4,832,881, 1989. (c) Aubert, J. H.; Sylwester, A. P. *Chemtech* 1991, April, 234-239.
(14) Stulikova, M. *J. Electroanal. Chem. Interfacial Electrochem.* **1973**, *48*, 33-45.
(15) Wang, J.; Martinez, T.; Yaniv, D. R.; McCormick, L. *J. Electroanal. Chem. Interfacial Electrochem.* **1990**, *286*, 265-272.
(16) Wojciechowski, M.; Balcerzak, J. *Anal. Chem* **1990**, *62*, 1325-1331.

RECEIVED for review July 9, 1991. Accepted October 8, 1991. This work was supported by grants from Sandia National Laboratories (under DOE Contract No. DE-ACO4-76DP00789) and the U.S. Environmental Protection Agency (Grant No. CR-817936-010). Mention of commercial products does not constitute endorsement by the U.S. EPA or the U.S. DOE. L.A. acknowledges a fellowship from Fundacão de Amparo á Pesquisa do Estado de São Paulo (FAPESP), Brazil.

Calibration of a Windowless Photoacoustic Cell for Detection of Trace Gases

György Z. Angeli* and Anikó M. Sólyom

Analtron Applied Research Company, POB 63, H-1311 Budapest, Hungary

András Miklós

Institute of Isotopes, Hungarian Academy of Sciences, POB 77, H-1525 Budapest, Hungary

Dane D. Bicanic

Laser Photoacoustic Laboratory, Department of Agricultural Engineering and Physics, Agricultural University, Duivendal 1, 6701 AP Wageningen, The Netherlands

The instrumental figure of performance, *F*, of a windowless, gas-phase photoacoustic cell, defined as the ratio of the normalized photoacoustic signal to the absorbance, is shown to be dependent on the sample, in contrast to previous assumptions. However, for a particular gas, *F* is independent of concentration in the ppm range. A method of calibration of such a cell is outlined in the absorbance range from 2×10^{-6} to 5×10^{-3}. The estimated detection limits at a signal to noise ratio of unity were 7.4 ppm, 0.43 ppb, and 1.3 ppb for carbon dioxide, ammonia, and ethylene, respectively.

INTRODUCTION

Photoacoustic (PA) spectroscopy is a sensitive method for the detection of gases at low concentration and as such appears to be a very attractive means of studying atmospheric pollution. The use of the photoacoustic (or, as it is often termed, the optoacoustic) effect, originally discovered by Bell (*1*), in combination with a strong laser infrared source was initially applied to detect weak absorption in gases (*2*). Technological developments in the field of lasers and high-sensitivity pressure detectors contributed to the substantial progress of photoacoustic spectroscopy (*3*, *4*). In recent years numerous studies have demonstrated the feasibility of infrared-laser photoacoustic spectroscopy in environmental applications and in agriculture (*5*–*11*). In our recent experiments a step tunable CO_2 laser radiation source—since its emission spectrum (9.4–10.6 μm) overlaps (*11*) with the absorption fingerprint of various pollutants—was used in conjunction with a windowless (open) resonant cell with a high acoustic quality factor designed for trace analysis of ambient air (*12*).

In the recently reported calibration procedure of the above-mentioned windowless cell, the PA system was considered as an analytical detector and the calibration itself was performed by conventional methods. In order to facilitate the comparison of various analytical PA systems, we suggest the introduction of a different quantity characterizing the PA instrument. This new parameter is consistent with the traditional terminology of analytical absorption spectroscopy, enabling direct comparison of PA spectroscopy with other spectroscopic methods.

Terminology. The intensity I_a absorbed by the sample can easily be calculated from Bouguer–Lambert–Beer's law as

$$I_a = I_0[1 - 10^{-A}] = I_t[10^A - 1] \quad (1)$$

where I_0 and I_t are the incident and transmitted powers, respectively (in watts), while A is absorbance. If $A \ll 1$, I_a can be approximated by a simpler expression:

$$I_a = I_t A \ln 10 \quad (2)$$

* Current address: Department of Chemistry, University of Arizona, Tucson, AZ 85721.

0003-2700/92/0364-0155$03.00/0

In several PA reports (*13–18*) the experimentally obtained plots of calibration curves were found to be linear. Theoretical calculation predicts the linearity of the signal response S (in volts) over the concentration range as broad as 7 orders of magnitude (*6*). We can therefore assume that the photoacoustic signal S is directly proportional to the absorbed radiation power I_a, i.e.

$$S \propto I_t A \ln 10 \tag{3}$$

In photoacoustic experiments the normalized microphone signal $S_N = S/I_t$ (volts per watt) is commonly measured. S_N is thus directly related to absorbance A by a proportionality factor known as the instrumental figure F (volts per watt) since

$$S_N = FA \tag{4}$$

The widely used parameter "cell constant" C (volt centimeters per watt) (*6*) is defined through

$$S = CI_t N\sigma \tag{5}$$

where N (number of moles per cubic centimeter) is the number of sample molecules in unit volume and σ (square centimeters) is the absorption cross section of the sample at the given wavelength. By comparison of the natural and common logarithmic form of Bouguer–Lambert–Beer's law, absorbance A can be calculated:

$$A = N\sigma d \log e \tag{6}$$

from which the relationship between C and F can be obtained:

$$F = C/d \ln 10 \tag{7}$$

where d (centimeters) is the interaction path length.

The quantity F can be expressed in terms of the physical parameters of the cell and the gas species using the cell constant relationship known from the literature (*6*), viz.

$$F = (c_p/c_v - 1)(G/V)(Q/\omega_1)R_M p_1 \ln 10 \tag{8}$$

where c_p and c_v represent specific heats of the given acoustic wave propagation substance at constant pressure and volume, G denotes a geometric factor, V is the volume of the cell, ω_1 is the acoustic resonance frequency, R_M represents the microphone sensitivity, and p_1 is the normalized pressure amplitude of the first acoustic mode at the location of the microphone.

In the parts per million concentration range (ppm) the contribution of the absorbing substance to the c_p and c_v values of the mixture is negligible compared to that of nitrogen. All other parameters in eq 8 are constant for the given experimental assembly.

For a multicomponent sample the calculation becomes more complicated due to different phases of photoacoustic signals generated by the individual constituents of the mixture (*7*).

EXPERIMENTAL SECTION

Laser. The laser was a homemade grating-tuned infrared CO_2 waveguide laser operating on a flowing mixture of helium, nitrogen, and carbon dioxide (18:3:1) at 75-mbar pressure in the plasma tube. In comparison with the conventional CO_2 laser, the waveguide laser is more compact (50-cm overall length) and has a much smaller bore (3 mm). The power output is typically of the order of several watts on more than 80 discrete laser transitions. The laser was equipped with a dither frequency stabilization system operated with the piezo bimorph plates mounted on the back of the grating. The laser power was monitored by a homemade PVDF foil thermal light detector and a lock-in amplifier (Type 128A, Princeton Applied Research, Princeton, NJ). The emitting transition of the laser was monitored by means of a CO_2 laser spectrum analyzer (Optical Engineering, Santa Rosa, CA).

Photoacoustic Cell. A windowless resonant photoacoustic cell manufactured from brass was provided with an electronic resonance locking circuitry which has been described in detail

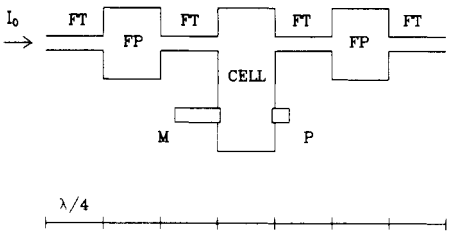

Figure 1. Longitudinal cross section of windowless acoustic chamber: (I_0) incident light; (FT) filter tubing; (M) microphone; (FP) filtering buffer; (P) piezo sound generator; (λ) acoustic wavelength.

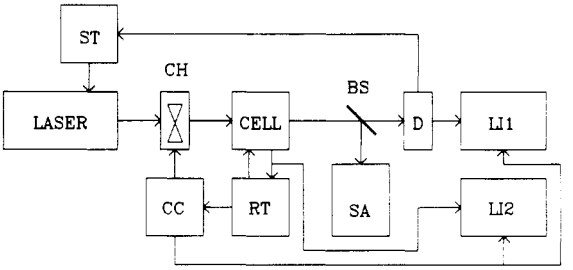

Figure 2. Experimental arrangement for CO_2 laser photoacoustic spectroscopy in conjunction with windowless cell: (ST) dither stabilization; (CH) chopper; (SA) spectrum analyzer; (BS) beam splitter; (D) PVDF light detector; (CC) chopper controller; (LI1, LI2) lock-in detectors; (RT) resonance tracking.

elsewhere (*19*). The cross section of the acoustic chamber is shown in Figure 1. Theoretically, the windowless cell design has the potential to considerably improve the detection sensitivity limit in the infrared region since neither the window material nor the gases adsorbed on the surface of the window could contribute to the generation of unwanted signals.

The chamber is essentially a cylinder provided with two small-diameter tubes, one on each side of the cylinder (Figure 1). The length of these tubes is the quarter of the acoustic wavelength of the resonance. They convert the soft acoustic termination of the ambient air at their open end to a high acoustic impedance at their chamber side; such an approach results in an almost perfect acoustic blocking of the cell, thus enabling cell operation at high quality factor (Q approximately 400). The first azimuthal resonant mode of the cylinder (close to 2 kHz) was excited by the absorbed energy. Additional suppression of the external acoustic noises was achieved by the specially designed additive acoustic filter system. A reasonable degree of vibrational insulation was obtained by packing the cell and the microphone in an aluminum container filled with polyurethane foam.

Electronic Resonance Locking System (ERLS). The acoustic amplification of the resonant chamber is a sensitive function of temperature and gas composition, since these influence the speed of sound and hence the resonance frequency. In order to eliminate the signal degradation due to the uncontrolled drifting of the cell's resonance frequency, we constructed active electronic circuitry capable of adjusting the chopper modulation frequency (*19*). Such an electronic resonance locking system (ERLS) was designed by taking advantage of the fact that the ratios of different mode frequencies of the cell are independent of gas composition as well as of the operating temperature. A longitudinal mode resonance peak of 4.67 kHz was selected, and an acoustic oscillator consisting of microphone, electronic amplifier, piezo sound generator, and the cell itself was built for that frequency. The ratio of the oscillator and the azimuthal resonance frequencies was examined carefully and a multiplier/divider circuit was constructed to tune the chopper frequency to the instantaneous resonance frequency of the cell.

Experimental Assembly. The schematic diagram of the experimental setup is shown in Figure 2. The amplitude modulation (2 kHz) was accomplished by means of a mechanical chopper in front of the laser output mirror. The chopper frequency was held on the given frequency by phase-lock-loop-like feedback circuitry. The acoustic signals were detected by a condenser microphone (Type 4176, Brüel and Kjaer, Naerum, Denmark) placed at the pressure maximum of the cell's first

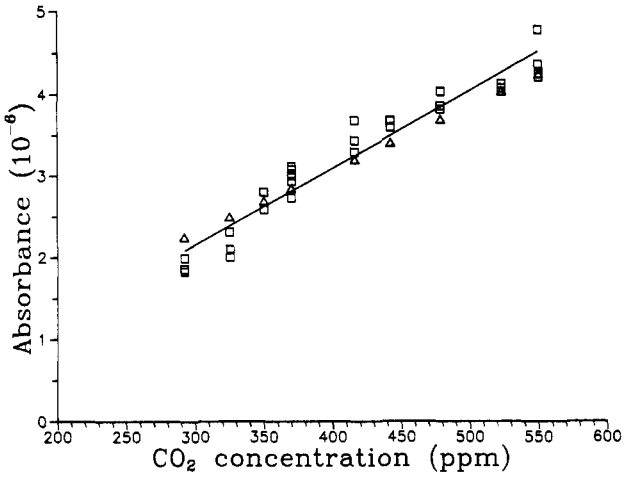

Figure 3. Absorbance versus concentration plot of carbon dioxide; (□) measured points; (△) calculated points.

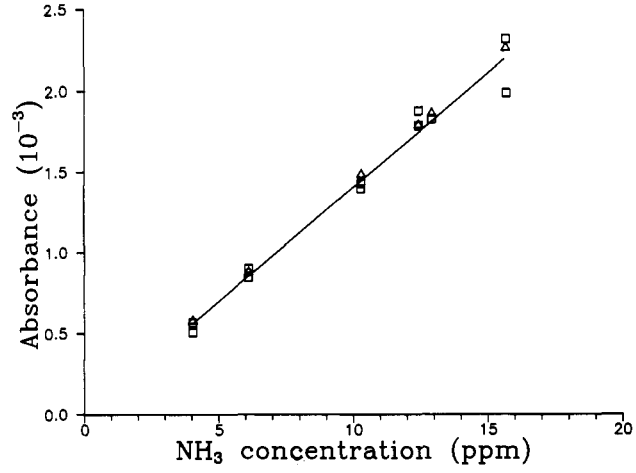

Figure 4. Absorbance versus concentration plot of ammonia: (□) measured points; (△) calculated points.

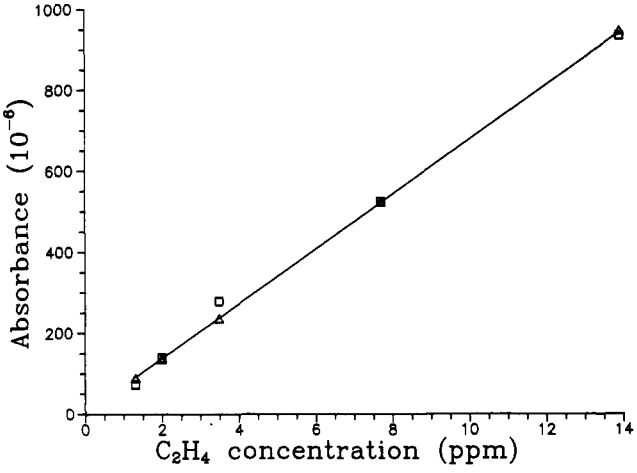

Figure 5. Absorbance versus concentration plot of ethylene: (□) measured points; (△) calculated points.

azimuthal mode. The sensitivity of the microphone was 50 mV/Pa under normal operating conditions. Following the preamplification (Type 2645, Brüel and Kjaer, Naerum, Denmark) the signal was fed into a lock-in amplifier (Type 3961, Ithaco, Ithaca, NY) equipped with a band-pass preamplifier with a quality factor of 5; the integration time was 10 s. The achieved noise level was 100 nV in all measurements. The filtered and amplified microphone signal was monitored by an oscilloscope. All amplitudes of the photoacoustic signal were registered on the chart recorder and normalized to the transmitted power of the laser.

Gas Handling. Gas mixtures were prepared from reagent grade gases and used without further purification. Very clean nitrogen (Hoekloos 5.0) was used as a diluting gas. Pure CO_2 (Hoekloos 9.8) served as one test gas. Certified precision gaseous mixtures of CO_2 (550 ppm, 348 ppmv) and C_4H_4 (136 ppm) in nitrogen were used (Hoekloos, The Netherlands); the NH_3 in nitrogen (100 ppmv) was provided by UCAR Specialty Gases (Union Carbide, Nieuw Vennep, The Netherlands). Further dilutions of these mixtures were carried out dynamically in the separate buffering reservoir before admission into the photoacoustic cell. The total flow rate of the mixtures was kept to below 1 l/min in order to eliminate the acoustic noise of the gas flow (*20*). The flow of each gas was controlled by means of a calibrated flow meter (Model 1355, Sho-Rate, Brooks Instrument, BV, Veenendaal, The Netherlands); all measurements were carried out with the cell at atmospheric pressure.

RESULTS

CO_2 Calibration. Mixtures containing 292–550 ppm and 8–12% carbon dioxide in nitrogen were studied at the 9R(16) laser line (9.29 μm). A plot of measured absorbance versus carbon dioxide concentration is shown in Figure 3. A linear least-squares fit to the measured data yields a correlation coefficient of 0.998 and a 7.4 ppm extrapolated detection limit at a signal to noise ratio of unity.

Ammonia Calibration. The dependence of the PA signal on the concentration of ammonia at the 9R(30) laser line (9.22 μm) was measured in the 1.5–15.7 ppm range. A plot of measured absorbance (Figure 4) versus the ammonia concentration for the data is linear (R coefficient 0.998), and the extrapolated detection limit corresponding to a signal to noise ratio of 1 is 0.43 ppb.

Ethylene Calibration. Measurements were made using sample concentrations varying between 1.3 and 13.9 ppm ethylene in nitrogen. As expected, the plot of the measured absorbance at the selected laser line 10P(14) (10.53 μm) versus ethylene concentrations (shown in Figure 5) exhibited a linear dependence with a correlation coefficient of 0.998 and a derived detection limit of 1.3 ppb.

Instrumental Figure. As stated above, mixtures of various composition were used to calibrate the system. The normalized photoacoustic signal was recorded; simultaneously, the magnitude of absorbance ($A_c = N\sigma d \log e$) was computed at each concentration using the literature data of the absorption cross sections (*21*). The measured data could be linearly fitted with high correlation factors. Obviously, the plot of measured absorbance versus concentration depends on the supposed value of the instrumental figure because, by definition, the measured absorbance is the ratio of S_N, the normalized photoacoustic signal, and F, the instrumental figure. The appropriate instrumental figure could be determined by minimizing the difference between the fitted curve and the computed absorbance values. The coincidence of the fitted and computed lines was calculated by the Student test. When this procedure was followed, the instrumental figures were determined independently for ethylene, ammonia, and carbon dioxide. The dependence of the instrumental figure on the gaseous species is displayed in Figure 6. The three instrumental figures were found to be different (with a significance of 99.9%): 0.98 V/W for carbon dioxide, 1.68 V/W for ethylene, and 2.4 V/W for ammonia. The instrumental figure of carbon dioxide was determined for the absorbance ranging from 1.9×10^{-6} to 4.6×10^{-6} and 0.62×10^{-3} to 0.93×10^{-3}, corresponding to the concentrations 292–550 and 8.1×10^4 to 12.0×10^4 ppm. The quality of the linear best fit was 98% (by the F test) in the entire concentration region (292 to 12.0×10^4 ppm). The gradient of the fitted curve was zero with very high significance.

CONCLUSIONS

Contrary to the reported literature data (*5*, *6*) and to eq 8, this research provides evidence that the instrumental figure

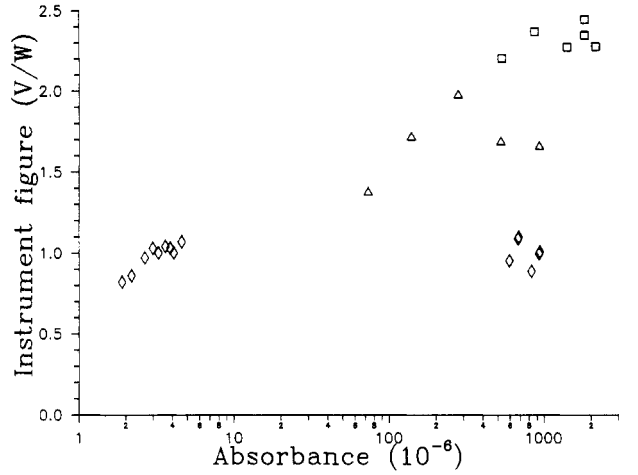

Figure 6. Dependence of instrumental figure F on absorbance of (◇) carbon dioxide, (□) ammonia, and (△) ethylene.

(related to the more familiar cell constant) is not independent of the absorbing gas. The cell constant cannot unambiguously be determined by a calibration measurement using a single absorbing species, indicating the "nonabsolute" character of photoacoustic spectroscopy. This implies that accurate and reliable results, similarly to other spectroscopic methods, can only be obtained through the appropriate standardization of our instrument for each sample material.

This experiment confirms the suitability of laser photoacoustic spectroscopy for accurate gas detection. The instrumental figure appears to be constant in a wide range of absorbances (concentrations); i.e. the calibration curves are straight lines—in good agreement with our original assumption. The absorbance as low as 2×10^{-6} could be measured with about 1 W of laser power and a coherent background level of 1 μV. The absorbance of 10^{-5} was measured by the differential optical absorption (DOAS) system (*22*), and the value of about 2×10^{-7} was achieved by the tunable diode laser spectroscopy (TDLS) (*23*).

In future experiments the amount of IR exciting power could be increased substantially (for example by using an intracavity arrangement). In addition, the level of unwanted background noise can further be reduced by means of acoustic and electronic filters (the background noise level exceeds that of electronic noise by 1 order of magnitude).

In conclusion, the concept of a windowless photoacoustic chamber was proved effective, a result that is in good agreement with the theoretical predictions and acoustic measurements (*19*). In general the detection limits achieved are comparable to or even better than those obtained for common closed cells. For ammonia, some published detection limits are 0.4 ppbv (*5*), 3 ppbv (*8*), and 1 ppbv (*7*). For ethylene, a characteristic detection limit is 0.7 ppbv (*6*). The long-term stability and the reproducibility of measurements were good, indicating the proper functioning of the electronic tracking system (ERLS). A unique advantage of the windowless design (apart from its potential to eliminate the unwanted window background) is its integrity and universality, since it allows the photoacoustic measurements across the virtually unlimited range of wavelengths without the need to replace the window or any other component.

ACKNOWLEDGMENT

We gratefully acknowledge the help received during the course of this study from Henk Jalink, Hans Sauren, and Cees van Asselt of the Department of Agricultural Engineering and Physics of the Wageningen Agricultural University. We are also grateful to Marcel Lubbers of the Department of Soil Science and Geology and Hillion Wegh of the Department of Air Pollution of Wageningen Agricultural University for their practical help and to Anton Janssen for his technical assistance.

Registry No. CO_2, 124-38-9; NH_3, 7664-41-7; C_2H_4, 74-85-1.

REFERENCES

(1) Bell, A. G. *Am. J. Sci.* **1880**, *19*, 305.
(2) Kreuzer, L. B. *Anal. Chem.* **1974**, *46*, 237A-244A.
(3) Rosencwaig, A. *Photoacoustics and Photoacoustic Spectroscopy*; Wiley Interscience: New York, 1980.
(4) Pao, Y. H. *Optoacoustic Spectroscopy and Detection*; Academic Press: New York, 1980.
(5) Sauren, H.; Bicanic, D. D.; Jalink, H.; Reuss, J. *J. Appl. Phys.* **1989**, *66*, 5085-5087.
(6) Meyer, P. L.; Sigrist, M. W. *Rev. Sci. Instrum.* **1990**, *61*, 1779-1807.
(7) Rooth, R. A.; Verhage, J. L.; Wouters, L. W. *Appl. Opt.* **1990**, *29*, 3643-3653.
(8) Sauren, H.; Bicanic, D. D.; van Asselt, C. *Infrared Phys.* **1991**, *31*, 475-484.
(9) Harren, F.; Reuss, J.; Woltering, E. J.; Bicanic, D. D. *Appl. Opt.* **1990**, *44*, 1360-1368.
(10) Sigrist, M. W.; Bernegger, S.; Meyer, P. L. *Infrared Phys.* **1989**, *29*, 805-814.
(11) Photoacoustic, Photothermal and Photochemical Processes in Gases. *Topics in Current Physics*; Hess, P., Ed.; Springer-Verlag: Berlin, 1989.
(12) Miklós, A.; Lörincz, A. *Appl. Phys. B* **1989**, *48*, 213.
(13) Kreuzer, L. B. *J. Appl. Phys.* **1971**, *42*, 2934-2943.
(14) Cvijin, Vujkovic, P.; Gilmore, D. A.; Atkinson, G. H. *Appl. Spectrosc.* **1988**, *42*, 770.
(15) Gilmore, D. A.; Oliphant, N.; Boutonnat, M.; Atkinson, G. H. *Anal. Chim. Acta* **1989**, *218*, 101-110.
(16) Boutonnat, M.; Gilmore, D. A.; Keilbach, K. A.; Oliphant, N.; Atkinson, G. H. *Appl. Spectrosc.* **1988**, *42*, 1519-1524.
(17) Vujkovic Cvijin, P.; Gilmore, D. A.; Leugers, M. A.; Atkinson, G. H. *Anal. Chem.* **1987**, *59*, 300-304.
(18) Leugers, M. A.; Atkinson, G. H. *Anal. Chem.* **1984**, *56*, 925-929.
(19) Angeli, Gy. Z.; Bozóki, Z.; Miklós, A.; Lörincz, A.; Thöny, A.; Sigrist, M. W. *Rev. Sci. Instrum.* **1991**, *62*, 810-813.
(20) Angeli, Gy. Z.; Miklós, A.; Sólyom, A. M.; Lörincz, A. *Acta Chim. Hung.*, in press.
(21) Bosher, J.; Schäfer, G.; Wiesemann, W. *Gasfernanalyse mit CO_2-Laser*; Batelle-Institute e.V.: Frankfurt, 1979.
(22) Finlayson Pitts, B. J.; Pitts, J. N., Jr. *Atmospheric Chemistry*; Wiley: New York, 1986.
(23) Carlisle, C. B.; Cooper, D. E. *Appl. Phys. Lett.* **1990**, *56*, 805-807.

RECEIVED for review June 1, 1991. Accepted October 8, 1991.